ACS APPLIED MATERIALS & INTERFACES

Research Article

www.acsami.org

Effects of Cyano-Substituents on the Molecular Packing Structures of Conjugated Polymers for Bulk-Heterojunction Solar Cells

Hyojung Cha,[†,‡] Hyoung Nam Kim,[‡,§] Tae Kyu An,[†] Moon Sung Kang,[⊥] Soon-Ki Kwon,*[,⊥] Yun-Hi Kim,*[,§] and Chan Eon Park*[,†]

[†]Department of Chemical Engineering, Pohang University of Science and Technology (POSTECH), Pohang, 790-784, Republic of Korea

[§]Department of Chemistry & Engineering Research Institute (ERI), and [⊥]School of Materials Science & Engineering, Engineering Research Institute (ERI), Gyeongsang National University, Jinju, 660-701, Republic of Korea

Supporting Information

ABSTRACT: The molecular packing structures of two conjugated polymers based on alkoxy naphthalene, one with cyano-substituents and one without, have been investigated to determine the effects of electron-withdrawing cyano-groups on the performance of bulk-heterojunction solar cells. The substituted cyano-groups facilitate the self-assembly of the polymer chains, and the cyano-substituted polymer:$PC_{71}BM$ blend exhibits enhanced exciton dissociation to $PC_{71}BM$. Moreover, the electron-withdrawing cyano-groups lower the highest occupied molecular orbital (HOMO) and lowest unoccupied molecular orbital (LUMO) levels of the conjugated polymer, which leads to a higher open circuit voltage (V_{OC}) and a lower energy loss during electron transfer from the donor to the acceptor. A bulk-heterojunction device fabricated with the cyano-substituted polymer:$PC_{71}BM$ blend has a higher V_{OC} (0.89 V), a higher fill factor (FF) (51.4%), and a lower short circuit current (J_{SC}) (7.4 mA/cm^2) than that of the noncyano-substituted polymer:$PC_{71}BM$ blend under AM 1.5G illumination with an intensity of 100 mW cm^{-2}. Thus, the cyano-substitution of conjugated polymers may be an effective strategy for optimizing the domain size and crystallinity of the polymer:$PC_{71}BM$ blend, and for increasing V_{OC} by tuning the HOMO and LUMO energy levels of the conjugated polymer.

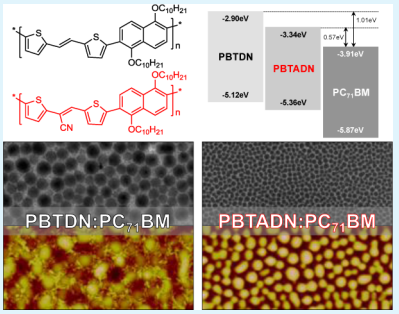

KEYWORDS: *electron-withdrawing cyano-groups, alkoxy naphthalene derivative, morphology control, conjugated polymer, phase separation, organic photovoltaics*

INTRODUCTION

One important feature of organic bulk heterojunction solar cells is their potential use in low-cost, printable photovoltaic devices. In addition, polymeric conjugated materials can be chemically tailored, which enables the synthesis of new photovoltaic materials.[1−10] Recently, the focus of research in this area has turned to donor−acceptor-type (D−A-type) conjugated polymers because of their low band gaps and good coverage of the solar spectrum.[1−8] By improving the molecular design of organic photovoltaics (OPVs), power conversion efficiencies of around 10% have been achieved.[7,8] The morphologies of the active layers of these high performance photovoltaic devices have been modified with various methods, including the introduction of solvent choice,[9] blend ratio,[10,11] processing additives,[12−14] annealing in solvents,[15,16] thermal annealing,[17,18] and the adoption of co-solvents[19,20] or orthogonal solvents.[14,15] Although various techniques for the fabrication of OPVs have been developed, research into the effects of molecular structure on device performance remains crucial. Novel materials with good solubility,[21,22] long wavelength absorption,[1−8] high charge mobility,[23] the appropriate energy levels,[24] lateral morphology,[25,26] vertical morphology,[27,28] long-term stability,[29] and that exhibit photoelectric conversion[30−32] in blends with fullerene derivatives are still required.

In general, a conjugated polymer has three components: the conjugated backbone, side chains, and substituents.[33] Although the electronic properties of conjugated polymers are very sensitive to the properties of the main chain, the substituents and side chains also affect their photovoltaic performances.[33] Substituent modification is often used as a method of fine-tuning the physical properties of conjugated polymers.[34−38] A recent trend in this area is the incorporation of electron-withdrawing substituents into the polymer structure, which can increase the V_{OC} of the associated solar cell.[34−38] The incorporation of an electron-withdrawing substituent is a simple and straightforward method for enhancing the π-conjugated structures of these materials through improved intermolecular packing and for fine-tuning their energy levels.[40−48] This strategy enables the examination of a range of morphologies and packing structures and their influence on the electronic properties of organic layers.

Received: May 7, 2014
Accepted: August 25, 2014
Published: August 25, 2014

Scheme 1. Synthetic Routes for the PBTDN and PBTADN Polymers

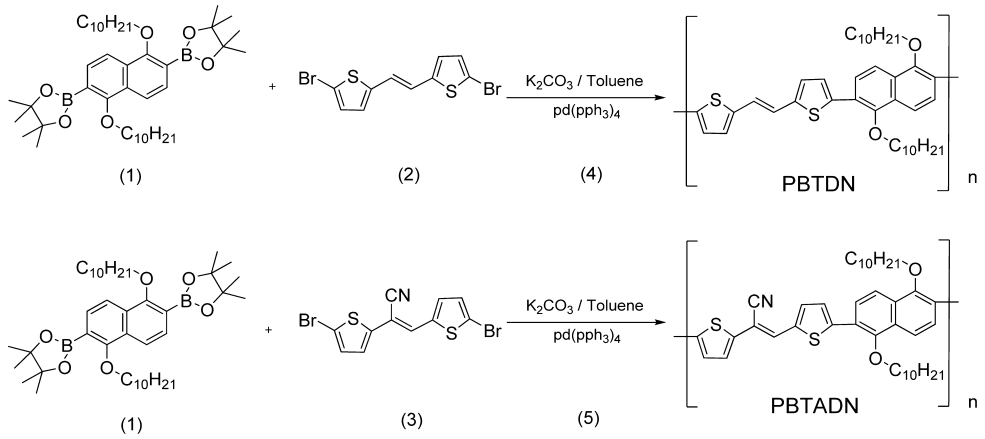

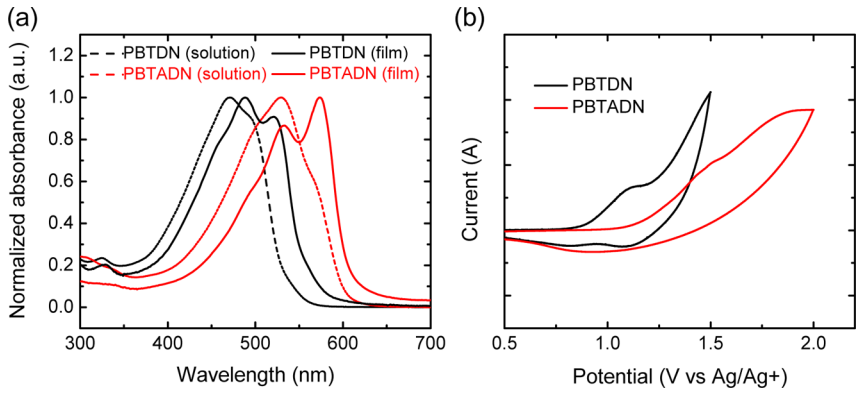

Figure 1. (a) Normalized absorption spectra of PBTDN and PBTADN in chlorobenzene solutions and thin films, and (b) cyclic voltammograms of PBTDN and PBTADN.

Table 1. Optical and Electrochemical Properties of the PBTDN and PBTADN Polymers

polymer	$\lambda_{abs\ max}$ (solution, nm)	$\lambda_{abs\ max}$ (film, nm)	$\lambda_{abs\ onset}{}^{a}$ (film, nm)	E_g^{opt} (eV)	E_{ox} (V)	HOMO (eV)	LUMO[b] (eV)
PBTDN	471	488	559	2.22	0.67	−5.12	−2.90
PBTADN	529	573	611	2.02	0.91	−5.36	−3.34

[a]Estimated from the onset of the absorption of each thin film. [b]Calculated from the optical band gap and the HOMO energy level of each polymer.

In this study, two alkoxy naphthalene based conjugated polymers containing two thiophenes and a vinylene linker, poly((5,5-E-a-((2-thienyl)methylene)-2-thiophene)-*alt*-2,6-[(1,5-didecyloxy)naphthalene])) (PBTDN) and poly((5,5-E-a-((2-thienyl)methylene)-2-thiopheneacetonitrile)-*alt*-2,6-[(1,5-didecyloxy)naphthalene])) (PBTADN)[39] (Scheme 1), were synthesized in order to assess the effects of electron-deficient cyano-substituents on the performances of the associated polymer solar cells. The molecular geometries and electronic structures of the two synthesized polymers were investigated with UV−visible spectroscopy, cyclic voltammetry (CV), density functional theory (DFT) quantum mechanics calculations, and grazing incidence wide-angle X-ray scattering (GIWAXS). Moreover, we investigated the effects of solvents on the molecular packing of the conjugated polymer blends with fullerene derivatives in bulk-heterojunction active layers without post-thermal treatment. The interpenetrated network morphologies of the bulk heterojunction layers were determined with atomic force microscopy (AFM) and transmission electron microscopy (TEM). The molecular geometries of the two synthesized polymers, PBTDN and PBTADN, and blends with $PC_{71}BM$ were investigated by GIWAXS.

RESULTS AND DISCUSSION

The structures and synthetic routes of the two copolymers PBTDN and PBTADN are shown in Scheme 1. The polymerizations were carried out with Suzuki coupling reactions.[39] The resulting PBTDN and PBTADN samples were found to be soluble in chloroform, chlorobenzene, dichlorobenzene, and toluene at room temperature. The good solubilities of these polymers enabled the preparation with solution processes of thin films for the fabrication of OPVs. Gel permeation chromatography (GPC) was performed in chloroform solution and analyzed relative to polystyrene standards. The PBTDN had a weight-average molecular weight (M_n) of 7700 g mol^{-1} with a polydispersity index (PDI) of 1.29. PBTADN had a M_n of 44 800 g mol^{-1} with a PDI of 1.46, as reported previously.[39] The structure of PBTDN was confirmed with ^1H NMR spectroscopy (see Figure S2 in the Supporting Information). The thermal stability of PBTDN was investigated by performing thermogravimetric analysis (TGA) at a heating rate of 10 °C min^{-1}. As shown in Figure S3 in the Supporting

Information, PBTDN exhibits 5 wt % thermal degradation above 370 °C, which indicates that the polymers are sufficiently thermally stable for use in solar cells. Our ^{1}H NMR spectroscopy and thermal degradation results for PBTADN have previously been presented;[39] 5 wt % thermal degradation occurs above 340 °C. The glass transitions of PBTDN and PBTADN occur at 142 and 200 °C, respectively.[39]

The UV−visible absorption properties of 10 mM PBTDN and PBTADN in chlorobenzene solution and in the thin film state were investigated, as shown in Figure 1a. The maximum absorption wavelengths (λ_{max}) and optical band gaps ($E_{g,opt}$) are summarized in Table 1. The high-energy absorption peaks (λ_{max}) of PBTDN and PBTADN in dilute solution are at 471 and 529 nm, respectively. The absorption maximum of PBTADN is red-shifted with respect to that of PBTDN, which is attributed to its greater π-conjugation length in the solution state. The UV−visible absorptions of as-cast thin films (approximately 110−130 nm) of PBTDN and PBTADN are bathochromically shifted with respect to those of the solution states by the strong intermolecular packing between aggregates.[51,52] The maximum absorption of the PBTADN film (λ_{max} = 573 nm) is red-shifted by approximately 85 nm with respect to that of the PBTDN film (λ_{max} = 488 nm). This difference means PBTADN will absorb light at longer wavelengths of the solar spectrum. The energy band gaps of PBTDN and PBTADN were calculated from extrapolation of the absorption edges and found to be around 2.22 and 2.02 eV, respectively. The above results are in good agreement with the π-conjugation and long-range ordering of PBTADN and the flexibility of PBTDN because of the absence of cyano-substituents.

The oxidation properties of PBTDN and PBTADN films were investigated with CV by using a platinum counter electrode in an acetonitrile solution containing 0.1 mol L^{-1} Bu_4NPF_6, and a scan rate of 50 mV s^{-1} (Figure 1b). A ferrocene reference value of −4.45 eV below the vacuum level was used in these measurements, and the energy level of the Ag/AgCl reference electrode was calibrated against the Fc/Fc$^+$ system and set at 4.45 eV by using previous methods.[39] The electrochemical properties are summarized in Table 1. The onset oxidation potentials ($E_{ox,onset}$) indicate that the highest occupied molecular orbital (HOMO) values of the PBTDN and PBTADN polymers are −5.12 and −5.36 eV, respectively. These results indicate that the presence of cyano-substituents decreases the HOMO level of PBTADN with respect to that of PBTDN.

The lowest unoccupied molecular orbital (LUMO) levels of PBTDN and PBTADN were determined from the calculated HOMO values and the optical band gaps to be −2.90 and −3.34 eV respectively. The LUMO energy levels of PBTDN and PBTADN were found to be approximately 1.01 and 0.57 eV higher respectively than the LUMO level (−3.91 eV) of $PC_{71}BM$ (see Figure 2),[53] which means that the electron transfer reactions are energetically favorable. It is well-known that a large difference between the LUMO energy levels of the donor and the acceptor increases the energy loss during electron transfer from the donor to the acceptor.[49]

To evaluate the oxidative and reductive properties of these polymers, the electronic properties of their dimer model compounds were calculated by using DFT quantum mechanics calculations. The HOMO and LUMO wave functions of the dimer model compounds are shown in Figure 3. All long alkyl chain substituents were replaced with methyl groups to simplify

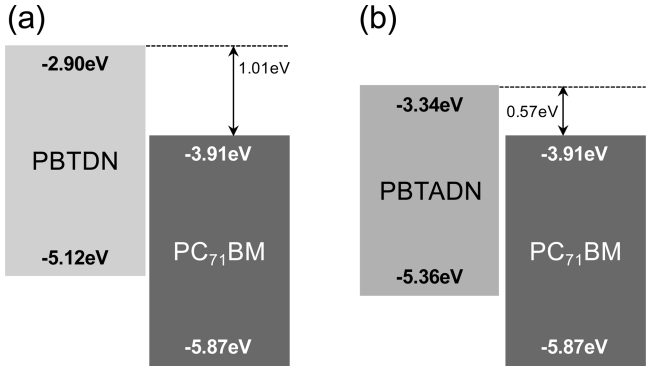

Figure 2. HOMO and LUMO energy levels of (a) a PBTDN:$PC_{71}BM$ blend and (b) a PBTADN:$PC_{71}BM$ blend.

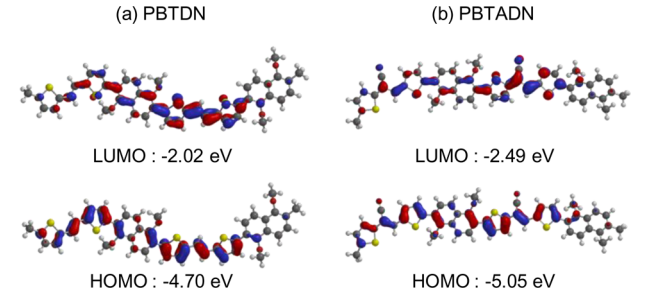

Figure 3. Molecular orbital surfaces of the HOMOs and LUMOs of the oligomers of (a) PBTDN and (b) PBTADN.

the calculations; this substitution only minimally affects the electronic properties.[54,55] The calculated electron densities of LUMO and HOMO in the PBTDN were localized over the region of the double bond between thiophenes in Figure 3a. However, those were delocalized along the conjugated backbone of PBTADN in Figure 3b. These results indicate that the intramolecular charge transfer along the main chain in PBTADN is effective when compared with the charge transfer in PBTDN. The LUMO and HOMO energy levels of PBTDN and PBTADN were found with these calculations to be −2.02 to −4.70 eV and −2.49 to −5.05 eV, respectively. Thus, the band gaps of PBTDN and PBTADN were determined to be 2.68 and 2.56 eV, respectively. The orderings of these results for the HOMOs, LUMOs, and band gaps of the two polymers are in agreement with those obtained with CV and UV−visible techniques. The calculated values differ somewhat from the corresponding experimental values, probably because the models contain only a handful of repeating units.[56,57] Our theoretical analyses of the electronic structures provide important insights into the differences between the electronic and optical properties of the two polymers.

The device with a 1:4 conjugated polymer to $PC_{71}BM$ weight ratio has the best PCE without postannealing treatment in Figure S4 and Tables S1 and S2 in the Supporting Information. The photovoltaic results obtained for the investigated blends under illumination of 100 mW cm^{-2} are summarized in Tables S3 and S4 in the Supporting Information. The current−voltage (J−V) curves in Figure 4 show that the performances of these 1:4 blend devices depend strongly on the solvent. The variations in the FF and PCE values of the solar cells containing PBTADN:$PC_{71}BM$ blends cast from CF, CB, and DCB are 50.3 to 51.5% and 3.0 to 3.4%, respectively; the variations in FF and PCE for the PBTDN:$PC_{71}BM$ blend solar

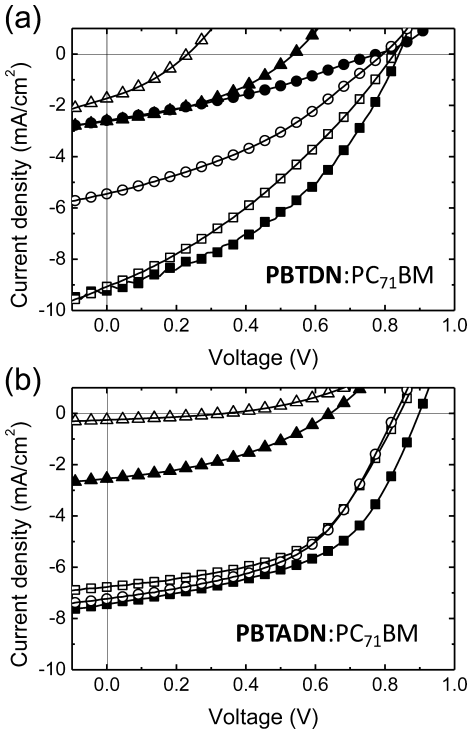

Figure 4. $J-V$ curves of ITO/PEDOT:PSS/polymer blend/LiF/Al devices under 100 mW/cm^2 illumination, where the polymer blends are (1:4) compositions of (a) PBTDN:PC$_{71}$BM and (b) PBTADN:PC$_{71}$BM cast from *o*-dichlorobenzene (■), chlorobenzene (□), tetrahydrofuran (●), chloroform (○), toluene (▲), and *p*-xylene (Δ).

cells are larger: 32.5 to 41.0% and 1.5 to 3.2%, respectively, which indicates that the presence of cyano-groups in PBTADN results in strong intermolecular interactions with the various solvents, as shown in Table 2. In addition, V_{OC} is determined

Table 2. Device Performances under 100 mW/cm^2 of PBTDN:PC$_{71}$BM (1:4) and PBTADN:PC$_{71}$BM (1:4) Blends Cast from DCB

	PBTDN:PC$_{71}$BM	PBTADN:PC$_{71}$BM
V_{OC} (V)	0.83	0.89
J_{SC} (mA cm^{-2})	9.2	7.4
FF (%)	41.0	51.4
PCE (%)	3.2	3.4
R_{SH} (Ω cm^2)	277	555
R_S (Ω cm^2)	31	29

by the donor/acceptor band-edge offset;[58] however, the electron-withdrawing cyano-substituent lowers the HOMO level below that of the noncyano-substituted polymer. Thus, the power conversion efficiency of the PBTADN:PC$_{71}$BM blend is expected to be higher than that of the PBTDN:PC$_{71}$BM blend because of the better properties of PBTADN.

AFM, TEM, and GIWAXS were performed to determine the molecular orderings of the polymer:PC$_{71}$BM blends. Each polymer:PC$_{71}$BM blend layer was prepared by spin-casting onto ITO glass with a deposited PEDOT:PSS film. Figure 5 shows AFM images of thin films of PBTDN:PC$_{71}$BM (1:4) and PBTADN:PC$_{71}$BM (1:4). The conjugated polymer:PC$_{71}$BM blend films cast from *p*-xylene (P-XL), toluene (TOL), and tetrahydrofuran (THF) have root-mean-square (rms) roughnesses of over 10 nm, which is associated with increased exciton recombination at D:A interface leading to poor excition dissociation and carrier extraction. In contrast, the films cast from chloroform (CF), chlorobenzene (CB), and *o*-dichlorobenzene (DCB) have morphologies with well-interpenetrated copolymer and PC$_{71}$BM materials, which may lead to better charge transport with increased shunt resistance, reduced series resistance, and high FF values.[59]

To examine these morphologies more closely, we obtained the TEM images shown in Figure 6 The dark regions in these TEM images are PCBM-rich domains, whereas the light regions are polymer-rich domains.[60,61] The PBTADN:PC$_{71}$BM blend film cast from CF solution has a smaller domain size, 20 (±10) nm, than the PBTDN:PC$_{71}$BM blend films. This is advantageous as most polymers have exciton diffusion lengths on the order of 10−20 nm.[62−64] PBTDN:PC$_{71}$BM blend films cast from CF contain large copolymer and PC$_{71}$BM domains, which diminish charge carrier transport and result in low FF values.[65] The well-interpenetrated morphologies of the conjugated polymer:PC$_{71}$BM blends cast from CB and DCB indicate that these films are expected to exhibit increased charge generation and more efficient charge collection in OPVs.[59] In particular, the PBTADN:PC$_{71}$BM blend film processed from DCB contains fibrillar polymer-rich domains and domain sizes of 10−20 nm. Such domain sizes and fibrillar structures in the active layer reduce charge recombination because evenly distributed morphological features provide defect-free contact with donor:acceptor interface or the metal cathode, which is related to lower resistance and increased FF values.[66−69] Such high contact area between the metal cathode and the fibrillar structures of donor which form longer and better connected pathways is of relevance for the electric characteristics of the contact, because a large interface allows a charge transfer over a large area and reduces the contact resistance.[66,67] The PBTDN:PC$_{71}$BM blend film cast from DCB solution also has the optimal domain size of 10 (±3) nm. However, it does not contain fibrillar structures or interconnected networks surrounded by continuous PC$_{71}$BM domains, which results in a higher level of nongeminate recombination of holes and electrons during device operation.[68,69]

The GIWAXS patterns of the pure polymer films were recorded and shown inFigure S5 in the Supporting Information. The GIWAXS pattern of the PBTADN film contains a clear peak, which is due to the molecular ordering and stacking of the conjugated polymer in the thin film. There is no peak observed for the PBTDN because of its amorphous behavior.

To gain insight into the organization of PBTDN and PBTADN in the conjugated polymer:PC$_{71}$BM blends, we performed GIWAXS on blend films cast from various solvents (Figure 7). According to the AFM and TEM images, the films cast from CB and DCB have bicontinuous structures. The GIWAXS pattern of the PBTADN:PC$_{71}$BM film contains a clear peak (d-spacing = 2.46 nm), except in the case of DCB, indicating that the ordering within the PDTADN regions is not fully disrupted by the presence of PCBM. On the basis of these observations, it is expected that the crystallinity of PBTADN may reduce nongeminate recombination.[70−72] The relative intensity variations of GIWAXS patterns of BTADN:PC$_{71}$BM between solvents is related to the phase separation between polymer and PCBM domain. Therefore, the remarkably large

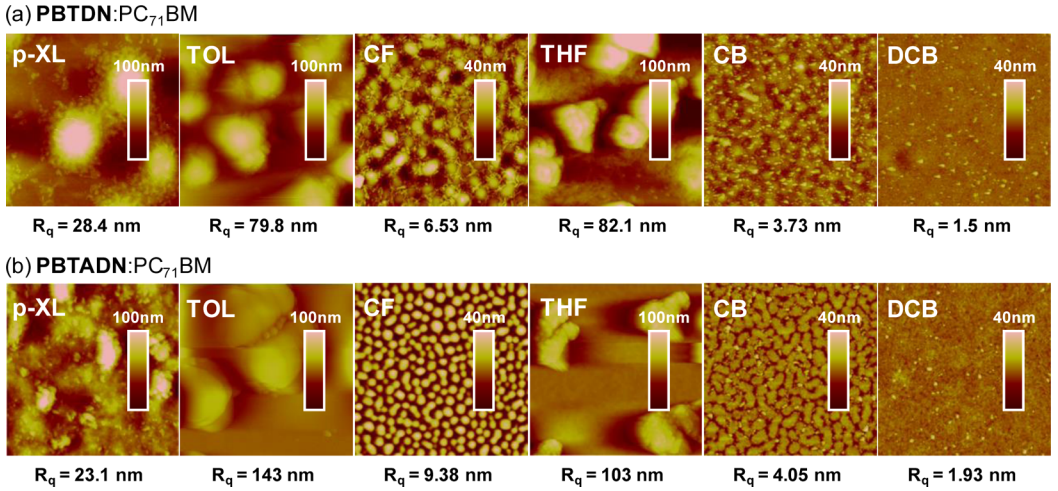

Figure 5. AFM images (5 μm × 5 μm) of (a) PBTDN:$PC_{71}BM$ and (b) PBTADN:$PC_{71}BM$ blend layers cast from various solvents.

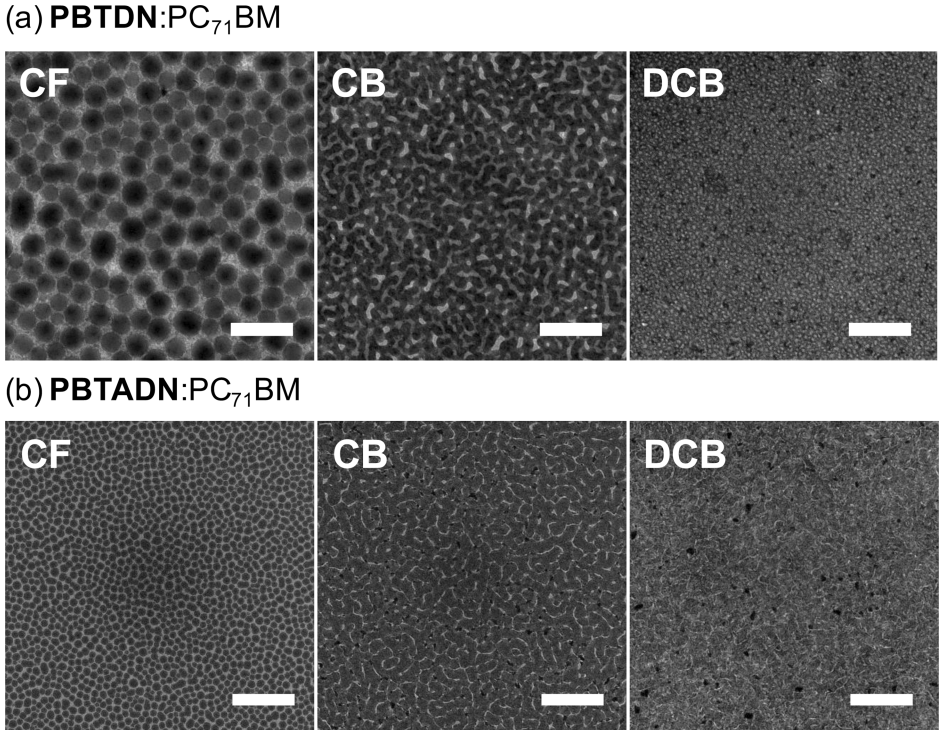

Figure 6. TEM images (5 μm × 5 μm) of (a) PBTDN:$PC_{71}BM$ and (b) PBTADN:$PC_{71}BM$ blend layers cast from various solvents.

separation of PBTADN:$PC_{71}BM$ with P-XL, TOL, and THF shows strong intensity of GIWAXS patterns.

On the other hand, the crystallinity of PBTADN results in larger phase separation than found in the PBTDN blend film, which increases geminate recombination at the interface of the D−A bulk heterojunction, and leads to a lower J_{SC} during device performance.[70−72]

The observed variation with the solvent in the PCEs of the PBTADN:$PC_{71}BM$ blend solar cells is believed to be due to the variation in the sizes of the polymer domains and $PC_{71}BM$ clusters, which affects the charge carrier transport from the polymer to $PC_{71}BM$. The PBTADN:$PC_{71}BM$ solar cells contain crystalline PBTADN and exhibit lower resistance due to their nanoscale morphologies and a higher degree of $\pi-\pi$ stacking than the PBTDN:$PC_{71}BM$ blend solar cells, which leads to higher FF values. Although both copolymer:$PC_{71}BM$ blends cast from the DCB solvent have the optimal domain size, the J_{SC} values of PBTDN and PBTADN are 9.2 and 7.4 mA/cm^2, respectively, as shown in Table 2. The crystalline polymer, PBTADN, has a larger domain size when cast from DCB than PBTDN, which means that it has a longer exciton dissociation length and increased geminate recombination.[50]

When switching to the electron-withdrawing group, a change in HOMO and LUMO levels would be expected.[40−48] In this investigation, by attaching cyano group on the vinylene part linking two thiophenes, the resulting polymer exhibited lower HOMO and LUMO levels, respectively, leading to a decreased band gap.[40−48,73] Moreover, this work clearly showed the effect of cyano substituent by modifying the interface of donor and acceptor bulk heterojunction and crystallinity between conjugated polymers.

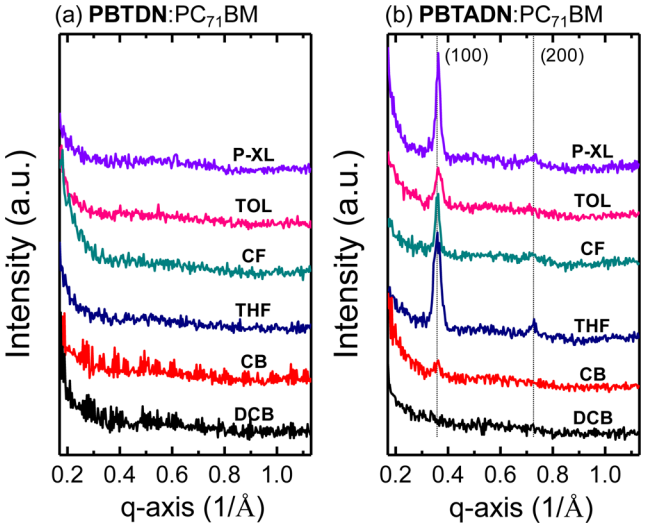

Figure 7. Out-of-plane GIWAXS patterns for (a) PBTDN:$PC_{71}BM$ and (b) PBTADN:$PC_{71}BM$ blend layers cast from various solvents.

CONCLUSIONS

In conclusion, two conjugated polymers based on alkoxy naphthalene, PBTDN and PBTADN, have been synthesized; PBTADN contains electron-withdrawing cyano-groups. PBTADN exhibits red-shifted light absorption properties that confirm the extension of π-conjugation and indicate long-range ordering. Moreover, PBTADN has a highly ordered molecular packing structure in the bulk state, and forms a fibrillar crystalline structure in its blends with $PC_{71}BM$, which reduces nongeminate charge recombination during solar cell operation. Furthermore, the electron-withdrawing cyano-groups lower the HOMO and LUMO energy levels of the conjugated polymer, which leads to high V_{OC} and decreases the energy loss during electron transfer from the donor to the acceptor. Although the J_{SC} values of the PBTADN:$PC_{71}BM$ blend solar cells are low, 7.4 mA/cm^2, the GIWAXS data of the PBTADN:$PC_{71}BM$ blends cast from CF, CB, and DCB indicate that the crystallinity of the cyano-substituted conjugated polymer is higher than that of PBTDN:$PC_{71}BM$, leading to the observed higher FF and PCE values of the solar cells.

EXPERIMENTAL METHOD

Materials. *n*-Butyllithium, 2-isopropoxy-3,3,4,4-tetramethyl-1,3,2-dioxaborolane, naphthalene-1,5-diol, bromine, iodine, potassium hydroxide, sodium iodide, titanium(IV) chloride, zinc, sodium carbonate, phenylboronic acid, 5-bromothiophene-2-carbaldehyde, and tetrakis(triphenylphosphine)-palladium were purchased from Aldrich Chemical Co.

Synthesis. *1. Synthesis of 2,6-(1′,2′-ethylborate)-1,5-didecyloxynaphthalene.* The synthesis was carried out according to an established method.[34] Yield: 35%, ^{1}H NMR (500 MHz, $CDCl_3$) [ppm] δ 7.94 (m, 2H), 7.76 (m, 2H), 4.08 (m, 4H), 1.96 (m, 4H), 1.59 (m, 4H), 1.41 (s, 24H), 1.37 (m, 24H), 0.91 (m, 6H), FT-IR (KBr, cm^{-1}): 3100 (aromatic C−H str), 2900 (aliphatic C−H str).

2. Synthesis of (E)-1,2-bis(5-bromothiophen-2-yl)ethene. Fifteen grams (78.50 mmol) of 5-bromothiophene-2-carbaldehyde and 12.2 g (188.4 mmol of zinc were added to 250 mL of anhydrous THF; 10.28 mL (94.2 mmol) of titanium(IV) chloride was slowly added to the mixture. The solution was stirred for 12 h at 60 °C. The crude product was recrystallized in ethanol. Yield: 30.6% (4.2 g). ^{1}HNMR (300 MHz, $CDCl_3$) [ppm] δ 6.96−6.95 (d, 2H), 6.82−6.78 (m, 4H). IR (KBr, cm^{-1}); 3030−3064 (aromatic CH).

3. Synthesis of (E)-2,3-bis(5-bromothiophen-2-yl)-acrylonitrile. The synthesis was carried out according to an established method.[38] The crude product was purified with column chromatography by using methylene dichloride as the eluent. Yield: 52% (4.7 g), ^{1}H NMR ($CDCl_3$, ppm) δ 7.27 (d, 1H), 7.26 (s, 1H), 7.10−7.07 (t, 2H), 7.02 (d, 1H), FT-IR (KBr, cm^{-1}): 3024 (aromatic C−H str), 2214 (nitrile C≡N str).

4. Synthesis of PBTDN. All handling of catalysts and polymerization was performed in a nitrogen atmosphere. To a stirred solution of 2,6-(1′,2′-ethylborate)-1,5-didecylxyloxy-naphthalene (1.97 g, 2.85 mmol) and (E)-1,2-bis(5-bromo-thiophen-2-yl)ethene (1 g, 2.85 mmol) in 10 mL 2 M K_2CO_3 solution in water was added the catalyst $Pd(PPh_3)_4$ (0.1 g, 0.008 mmol %). The reaction mixture was heated at 80 °C under nitrogen for 48 h. Bromobenzene (0.005 g, 0.0318 mmol) was added and then phenyl boronic acid (0.005 g, 0.041 mmol) was added with small amounts of catalysts for end-capping. After 2 h, the reaction mixture was poured into methanol (50 mL) and filtered with a glass filter. The residue was dissolved in $CHCl_3$ and washed with water. The precipitation was repeated twice with chloroform/methanol. Yield: 52%, ^{1}H NMR (300 MHz, $CDCl_3$) [ppm] δ 8.05−7.72 (m, 4H), 7.57−7.56 (d, 2H), 7.21−7.08 (m, 4H), 3.97(d, 4H), 2.02−2.00 (m, 4H), 1.42−1.08 (m, 28H), 0.90−0.88 (m, 6H), FT-IR (KBr, cm^{-1}): 3100−3066 (aromatic C−H str), 2921−2849 (aliphatic C−H str).

5. Synthesis of PBTADN. The polymer was prepared via a palladium-catalyzed Suzuki coupling reaction according to an established method.[39]

Characterization. The ^{1}H NMR spectra were recorded on a Bruker 300 MHz NMR spectrometer and the results are expressed in ppm relative to the internal standard. The FT-IR spectra were obtained with a Bomem Michelson series FT-IR spectrometer. The UV−vis absorption spectra were obtained in chloroform with a Shimadzu UV 3100 spectrometer. The molecular weights and polydispersities of the polymers were determined by performing gel permeation chromatography (GPC) analysis with polystyrene standard calibration (Waters high pressure GPC assembly model M590 pump μ-Styragel columns of 105, 104, 103, 500, and 100 Å, refractive index detectors, solvent $CHCl_3$). TGA measurements were performed on a PerkinElmer series 7 analysis system under N_2 at a heating rate of 10 °C/min. Cyclic voltammetry was carried out in a two-compartment cell with platinum electrodes at a scan rate of 10 mV/s against an Ag/Ag+ (0.1 M $AgNO_3$ in acetonitrile) reference electrode in an anhydrous and nitrogen-saturated solution of 0.1 M Bu_4NBF_4 in acetonitrile. Molecular orbital surfaces of polymers were obtained by using the Spartan 08 program with the ab initio Hartree−Fock (HF) and density functional theory (DFT-B3LYP) methods and the 6-311G* and 6-3111G** basis sets.

The current density−voltage (J−V) characteristics were measured by using a Keithley 4200 source measurement unit in the dark and under AM 1.5G solar illumination (Oriel 1 kW solar simulator) with respect to a reference cell PVM 132 calibrated at the National Renewable Energy Laboratory at an intensity of 100 mW/cm^2. UV−visible (Cary:Varian Co.) measurements were used to analyze the optical properties of the conjugated polymer:$PC_{71}BM$ blend layers. Atomic force

microscopy (AFM) (Multimode IIIa, Digital Instruments) was performed in tapping mode to acquire images of the surfaces of the conjugated polymer:$PC_{71}BM$ blend layers. For the transmission electron microscopy (TEM) investigation, the conjugated polymer:$PC_{71}BM$ layers were floated from the water-soluble PEDOT:PSS substrates onto the surface of dematerialized water and picked up with 200-mesh copper TEM grids. TEM images were obtained by using a HITACHI-7600 operated at 100 kV. Grazing incidence out-of-plane X-ray diffraction experiments were performed at the 5A beamline (λ = 1.54 Å) at the Pohang Accelerator Laboratory, Pohang, Korea.[74] Total external reflection angle of GIWAXS measurements is 0.14° to unify the penetration depth of thin films. Six circle diffractormenter and scintillation detector are used to control external reflection angle with no calibration standard. The exposure time was 1 s at each measured angles.

Device Fabrication. Organic solar cells were fabricated using the conjugated polymers as electron donors and the fullerene derivative $PC_{71}BM$ as the electron acceptor. The conjugated polymers PBTDN and PBTADN were synthesized via palladium-catalyzed Suzuki coupling reactions, as described above. $PC_{71}BM$ (99.5%) was obtained from Nano-C, Inc. Twenty mg/mL solutions of the conjugated polymer and fullerene derivative in dichlorobenzene were prepared and stirred in a glovebox at 80 °C under a nitrogen atmosphere overnight. Glass substrates prepatterned with indium tin oxide (ITO) were cleaned in a sonic bath of detergent solution, followed by rinsing with D.I. water, acetone, and 2-propanol. Immediately after 20 min of UV/ozone treatment, thin layers of poly(3,4-ethylenedioxythiophene):polystyrenesulfonate (PEDOT:PSS; Bay P VP AI4083, Bayer AG) for hole injection were spin coated to form 30−40 nm thick films on the cleaned ITO-patterned glass substrates after filtration with a 0.45 μm PVDF filter. The blend solutions were spin-coated at 1000 rpm for 60 s (see Table S5 in the Supporting Information) to a thickness of 100−200 nm on top of the PEDOT:PSS layers after filtration with a 0.2 μm PTFE filter for all solvents. The LiF and Al cathodes were thermally deposited to thicknesses of 1 and 100 nm, respectively, onto the surfaces of the active layers.

■ ASSOCIATED CONTENT

Supporting Information

^{1}H NMR spectrum, DSC, and TGA of the PBTDN polymer; concentration and thickness of polymer:$PC_{71}BM$ films; device performance of polymer:PCBM blend with different ratios, thermal annealing temperatures, and organic solvent; and out-of-plane GIWAXS patterns for polymer:$PC_{71}BM$. This material is available free of charge via the Internet at http://pubs.acs.org/.

■ AUTHOR INFORMATION

Corresponding Authors

*E-mail: skwon@gnu.ac.kr.
*E-mail: ykim@gnu.ac.kr.
*E-mail: cep@postech.ac.kr.

Author Contributions

‡H.C. and H.N.K. contributed equally.

Notes

The authors declare no competing financial interest.

■ ACKNOWLEDGMENTS

This study was supported by grants from the Basic Science Research Program (2014R1A2A1A05004993 & 2012R1A2A2A06047047) and the Center for Advanced Soft Electronics under the Global Frontier Research Program (2011-0031639 & 2013M3A6A5073172) through the National Research Foundation funded by the Ministry of Education, Science and Technology (Korea).

■ REFERENCES

(1) Chen, H.-Y.; Hou, J.; Zhang, S.; Liang, Y.; Yang, G.; Yang, Y.; Yu, L.; Wu, Y.; Li, G. Polymer Solar Cells with Enhanced Open-Circuit Voltage and Efficiency. *Nat. Photonics* **2009**, *3*, 649−653.

(2) Service, R. F. Outlook Brightens for Plastic Solar Cells. *Science* **2011**, *332*, 293−293.

(3) Green, M. A.; Emery, K.; Hishikawa, Y.; Warta, W. Progress in Photovoltaics: Research and Applications. *Prog. Photovoltaics* **2011**, *19*, 84−92.

(4) He, Z.; Zhong, C.; Huang, X.; Wong, W.-Y.; Wu, H.; Chen, L.; Su, S.; Cao, Y. Simultaneous Enhancement of Open-Circuit Voltage, Short-Circuit Current Density, and Fill Factor in Polymer Solar Cells. *Adv. Mater.* **2011**, *23*, 4636−4643.

(5) Dou, L.; You, J.; Yang, J.; Chen, C.-C.; He, Y.; Murase, S.; Moriarty, T.; Emery, K.; Li, G.; Yang, Y. Tandem Polymer Solar Cells Featuring a Spectrally Matched Low-Bandgap Polymer. *Nat. Photonics* **2012**, *6*, 180−185.

(6) You, J.; Dou, L.; Yoshimura, K.; Kato, T.; Ohya, K.; Moriarty, T.; Emery, K.; Chen, C. C.; Gao, J.; Li, G.; Yang, Y. A Polymer Tandem Solar Cell with 10.6% Power Conversion Efficiency. *Nat. Commun.* **2013**, *4*, 1446−1455.

(7) He, Z.; Zhong, C.; Su, S.; Xu, M.; Wu, H.; Cao, Y. Enhanced Power-Conversion Efficiency in Polymer Solar Cells using an Inverted Device Structure. *Nat. Photonics* **2012**, *6*, 591−595.

(8) Heliatek Consolidates its Technology Leadership by Establishing a New World Record for Organic Solar Technology with a Cell Efficiency of 12%. http://www.heliatek.com/newscenter/latest_news/neuer-weltrekord-fur-organische-solarzellen-heliatek-behauptet-sich-mit-12-zelleffizienz-als-technologiefuhrer/?lang=en (accessed March 2013).

(9) Kim, Y. S.; Lee, Y.; Kim, J. K.; Seo, E.-O.; Lee, E.-W.; Lee, W.; Han, S.-H.; Lee, S.-H. Effect of Solvents on the Performance and Morphology of Polymer Photovoltaic Devices. *Curr. Appl. Phys.* **2010**, *10*, 985−989.

(10) Wang, T.; Dunbar, A. D. F.; Staniec, P. A.; Pearson, A. J.; Hopkinson, P. E.; MacDonald, J. E.; Lilliu, S.; Pizzey, C.; Terrill, N. J.; Donald, A. M.; Ryan, A. J.; Jones, R. A. L.; Lidzey, D. G. The Development of Nanoscale Morphology in Polymer:Fullerene Photovoltaic Blends during Solvent Casting. *Soft Matter* **2010**, *6*, 4128−4134.

(11) Schmidt-Hansberg, B.; Klein, M. F.G.; Munuera, C.; Vorobiev, A.; Colsmann, A.; Scharfer, P.; Lemmer, U.; Schabel, W.; Dosch, H.; Barrena, E. Effect of Photovoltaic Polymer/Fullerene Blend Composition Ratio onMicrostructure Evolution during Film Solidification Investigated in Real Time by X-ray Diffraction. *Macromolecules* **2011**, *44*, 3795−3800.

(12) Peet, J.; Kim, J. Y.; Coates, N. E.; Ma, W. L.; Moses, D.; Heeger, A. J.; Bazan, G. C. Efficiency Enhancement in Low-Bandgap Polymer Solar Cells by Processing with Alkane Dithiols. *Nat. Mater.* **2007**, *6*, 497−500.

(13) Lee, J. K.; Ma, W. L.; Brabec, C. J.; Yuen, J.; Moon, J. S.; Kim, J. Y.; Lee, K.; Bazan, G. C.; Heeger, A. J. Processing Additives for Improved Efficiency from Bulk Heterojunction Solar Cells. *J. Am. Chem. Soc.* **2008**, *130*, 3619−3623.

(14) An, T. K.; Kang, I.; Yun, H.-J.; Cha, H.; Hwang, J.; Park, S.; Kim, J.; Kim, Y. J.; Chung, D. S.; Kwon, S.-K.; Kim, Y.-H.; Park, C. E. Solvent Additive to Achieve Highly Ordered Nanostructural Semicrystalline DPP Copolymers: Toward a High Charge Carrier Mobility. *Adv. Mater.* **2013**, *25*, 7003−7009.

(15) Li, G.; Shrotriya, V.; Huang, J.; Yao, Y.; Moriarty, T.; Emery, K.; Yang, Y. High-Efficiency Solution Processable Polymer Photovoltaic Cells by Self-Organization of Polymer Blends. *Nat. Mater.* **2005**, *4*, 864−868.
(16) Park, J. H.; Kim, J. S.; Lee, J. H.; Lee, W. H.; Cho, K. Effect of Annealing Solvent Solubility on the Performance of Poly(3-hexylthiophene)/Methanofullerene Solar Cells. *J. Phys. Chem. C* **2009**, *113*, 17579−17584.
(17) Padinger, F.; Rittberger, R. S.; Sariciftci, N. S. Effects of Postproduction Treatment on Plastic Solar Cells. *Adv. Funct. Mater.* **2003**, *13*, 85−88.
(18) McNeill, C. R.; Halls, J. J. M.; Wilson, R.; Whiting, G. L.; Berkebile, S.; Ramsey, M. G.; Friend, R. H.; Greenham, N. C. Efficient Polythiophene/Polyfluorene Copolymer Bulk Heterojunction Photovoltaic Devices: Device Physics and Annealing Effects. *Adv. Funct. Mater.* **2008**, *18*, 2309−2321.
(19) Park, S. H.; Roy, A.; Beaupre, S.; Cho, S.; Coates, N.; Moon, J. S.; Moses, D.; Leclerc, M.; Lee, K.; Heeger, A. J. Bulk Heterojunction Solar Cells with Internal Quantum Efficiency Approaching 100%. *Nat. Photonics* **2009**, *3*, 297−302.
(20) Rochester, C. W.; Mauger, S. A.; Moulé, A. J. Investigating the Morphology of Polymer/Fullerene Layers Coated Using Orthogonal Solvents. *J. Phys. Chem. C* **2012**, *116*, 7287−7292.
(21) Cheng, Y.-J.; Yang, S.-H.; Hsu, C.-S. Synthesis of Conjugated Polymers for Organic Solar Cell Applications. *Chem. Rev.* **2009**, *109*, 5868−5923.
(22) Gunes, S.; Neugebauer, H.; Sariciftci, N. S. Conjugated Polymer-Based Organic Solar Cells. *Chem. Rev.* **2007**, *107*, 1324−1338.
(23) Cha, H.; Lee, G. Y.; Fu, Y.; Kim, Y. J.; Park, C. E.; Park, T. Simultaneously Grasping and Self-Organizing Photoactive Polymers for Highly Reproducible Organic Solar Cells with Improved Efficiency. *Adv. Energy Mater.* **2013**, *3*, 1018−1024.
(24) Cha, H.; Chung, D. S.; Bae, S. Y.; Lee, M.-J.; An, T. K.; Hwang, J.; Kim, K. H.; Kim, Y.-H.; Choi, D. H.; Park, C. E. Complementary Absorbing Star-Shaped Small Molecules for the Preparation of Ternary Cascade Energy Structures in Organic Photovoltaic Cells. *Adv. Funct. Mater.* **2013**, *23*, 1556−1565.
(25) Blouin, N.; Michaud, A.; Leclerc, M. A Low-Bandgap Poly(2,7-Carbazole) Derivative for Use in High-Performance Solar Cells. *Adv. Mater.* **2007**, *19*, 2295−2300.
(26) Wang, T.; Pearson, A. J.; Dunbar, A. D. F.; Staniec, P. A.; Watters, D. C.; Yi, H.; Ryan, A. J.; Jones, R. A. L.; Iraqi, A.; Lidzey, D. G. Correlating Structure with Function in Thermally Annealed PCDTBT:PC70BM Photovoltaic Blends. *Adv. Funct. Mater.* **2012**, *22*, 1399−1408.
(27) Subbiah, J.; Amb, C. M.; Reynolds, J. R.; So, F. Effect of Vertical Morphology on the Performance of Silole-Containing Low-Bandgap Inverted Polymer Solar Cells. *Sol. Energy Mater. Sol. C* **2012**, *97*, 97−101.
(28) Rice, A. H.; Giridharagopal, R.; Zheng, S. X.; Ohuchi, F. S.; Ginger, D. S.; Luscombe, C. K. Controlling Vertical Morphology within the Active Layer of Organic Photovoltaics using Poly(3-hexylthiophene) Nanowires and Phenyl-C61-Butyric Acid Methyl Ester. *ACS Nano* **2011**, *5*, 3132−3140.
(29) Brabec, C. J.; Cravino, A.; Meissner, D.; Sariciftci, N. S.; Fromherz, T.; Minse, M.; Sanchez, L.; Hummelen, J. C. Origin of the Open Circuit Voltage of Plastic Solar Cells. *Adv. Funct. Mater.* **2001**, *11*, 374−380.
(30) Dolores Perez, M.; Borek, C.; Forrest, S. R.; Thompson, M. E. Molecular and Morphological Influences on the Open Circuit Voltages of Organic Photovoltaic Devices. *J. Am. Chem. Soc.* **2009**, *131*, 9281−9286.
(31) Cowan, S. R.; Roy, A.; Heeger, A. J. Recombination in Polymer-Fullerene Bulk Heterojunction Solar Cells. *Phys. Rev. B* **2010**, *82*, 245207−10.
(32) Deibel, C.; Strobel, T.; Dyakonov, V. Role of the Charge Transfer State in Organic Donor−Acceptor Solar Cells. *Adv. Mater.* **2010**, *22*, 4097−4111.
(33) Zhou, H.; Yang, L.; You, W. Rational Design of High Performance Conjugated Polymers for Organic Solar Cells. *Macromolecules* **2012**, *45*, 607−632.
(34) Brédas, J. L.; Heeger, A. J. Influence of Donor and Acceptor Substituents on the Electronic Characteristics of Poly(paraphenylene vinylene) and Poly(paraphenylene). *Chem. Phys. Lett.* **1994**, *217*, 507−512.
(35) Stuart, A. C.; Tumbleston, J. R.; Zhou, H.; Li, W.; Liu, S.; Ade, H.; You, W. Fluorine Substituents Reduce Charge Recombination and Drive Structure and Morphology Development in Polymer Solar Cells. *J. Am. Chem. Soc.* **2013**, *135*, 1806−1815.
(36) Huang, Y.; Hou, L.; Zhang, S.; Guo, X.; Han, C. C.; Li, Y.; Hou, J. Sulfonyl: a New Application of Electron-Withdrawing Substituent in Highly Efficient Photovoltaic Polymer. *Chem. Commun.* **2011**, *47*, 8904−8906.
(37) Son, H. J.; Wang, W.; Xu, T.; Liang, Y.; Wu, Y.; Li, G.; Yu, L. Synthesis of Fluorinated Polythienothiophene-co-benzodithiophenes and Effect of Fluorination on the Photovoltaic Properties. *J. Am. Chem. Soc.* **2011**, *133*, 1885−1894.
(38) Jeong, H.-G.; Khim, D.; Jung, E.; Yun, J.-M.; Kim, J.; Ku, J.; Jang, Y. H.; Kim, D.-Y. Synthesis and Characterization of a Novel Ambipolar Polymer Semiconductor based on a Fumaronitrile Core as an Electron-Withdrawing Group. *J. Polym. Sci., Part A: Polym. Chem.* **2013**, *51*, 1029−1039.
(39) Kwon, J. H.; An, J.-Y.; Jang, H.; Choi, S.; Chung, D. S.; Lee, M.-J.; Cha, H.; Park, J.-H.; Park, C.-E.; Kim, Y.-H. Development of a New Conjugated Polymer Containing Dialkoxynaphthalene for Efficient Polymer Solar Cells and Organic Thin Film Transistors. *J. Polym. Sci., Part A: Polym. Chem.* **2011**, *49*, 1119−1128.
(40) Schroeder, B. C.; Huang, Z.; Shahid Ashraf, R.; Smith, J.; D'Angelo, P.; Watkins, S. E.; Anthopoulos, T. D.; Durrant, J. R.; McCulloch, I. Silaindacenodithiophene-Based Low Band Gap Polymers−The Effect of Fluorine Substitution on Device Performances and Film Morphologies. *Adv. Funct. Mater.* **2012**, *22*, 1663−1670.
(41) Haid, S.; Mishra, A.; Weil, M.; Uhrich, C.; Pfeiffer, M.; Bäuerle, P. Synthesis and Structure−Property Correlations of Dicyanovinyl-Substituted Oligoselenophenes and their Application in Organic Solar Cells. *Adv. Funct. Mater.* **2012**, *22*, 4322−4333.
(42) Wong, W. W. H.; Singh, T. B.; Vak, D.; Pisula, W.; Yan, C.; Feng, X.; Williams, E. L.; Chan, K. L.; Mao, Q.; Jones, D. J.; Ma, C.-Q.; Müllen, K.; Bäuerle, P.; Holmes, A. B. Solution Processable Fluorenyl Hexa-*peri*-hexabenzocoronenes in Organic Field-Effect Transistors and Solar Cells. *Adv. Funct. Mater.* **2010**, *20*, 927−938.
(43) Bartelt, J. A.; Douglas, J. D.; Mateker, W. R.; Labban, A. E.; Tassone, C. J.; Toney, M. F.; Fréchet, J. M. J.; Beaujuge, P. M.; McGehee, M. D. Controlling Solution-Phase Polymer Aggregation with Molecular Weight and Solvent Additives to Optimize Polymer-Fullerene Bulk Heterojunction Solar Cells. *Adv. Energy Mater.* **2014**, DOI: 10.1002/aenm.201301733.
(44) Zhou, H.; Yang, L.; Stuart, A. C.; Price, S. C.; Liu, S.; You, W. Development of Fluorinated Benzothiadiazole as a Structural Unit for a Polymer Solar Cell of 7% Efficiency. *Angew. Chem., Int. Ed.* **2011**, *50*, 2995−2998.
(45) Li, W.; Yang, L.; Tumbleston, J. R.; Yan, L.; Ade, H.; You, W. Controlling Molecular Weight of a High Efficiency Donor-Acceptor Conjugated Polymer and Understanding Its Significant Impact on Photovoltaic Properties. *Adv. Mater.* **2014**, DOI: 10.1002/adma.201305251.
(46) Yang, L.; Tumbleston, J. R.; Zhou, H.; Ade, H.; You, W. Disentangling the Impact of Side Chains and Fluorine Substituents of Conjugated Donor Polymers on the Performance of Photovoltaic Blends. *Energy Environ. Sci.* **2013**, *6*, 316−326.
(47) Bronstein, H.; Frost, J. M.; Hadipour, A.; Kim, Y.; Nielsen, C. B.; Shahid Ashraf, R.; Rand, B. P.; Watkins, S.; McCulloch, I. Effect of Fluorination on the Properties of a Donor−Acceptor Copolymer for Use in Photovoltaic Cells and Transistors. *Chem. Mater.* **2013**, *25*, 277−285.

(48) Stuart, A. C.; Tumbleston, J. R.; Zhou, H.; Li, W.; Liu, S.; Ade, H.; You, W. Fluorine Substituents Reduce Charge Recombination and Drive Structure and Morphology Development in Polymer Solar Cells. *J. Am. Chem. Soc.* **2013**, *135*, 1806−1815.
(49) Li, G.; Nitzan, A.; Ratner, M. A. Yield of Exciton Dissociation in a Donor−Acceptor Photovoltaic Junction. *Phys. Chem. Chem. Phys.* **2012**, *14*, 14270−14276.
(50) Credgington, D.; Jamieson, F. C.; Walker, B.; Nguyen, T.-Q.; Durrant, J. R. Quantification of Geminate and Non-Geminate Recombination Losses within a Solution-Processed Small-Molecule Bulk Heterojunction Solar Cell. *Adv. Mater.* **2012**, *24*, 2135−2141.
(51) Würthner, F.; Kaiser, T. E.; Saha-Möller, C. R. J-Aggregates: From Serendipitous Discovery to Supramolecular Engineering of Functional Dye Materials. *Angew. Chem., Int. Ed.* **2011**, *50*, 3376−3410.
(52) Deing, K. C.; Mayerhöffer, U.; Würthner, F.; Meerholz, K. Aggregation-Dependent Photovoltaic Properties of Squaraine/$PC_{61}BM$ Bulk Heterojunctions. *Phys. Chem. Chem. Phys.* **2012**, *14*, 8328−8334.
(53) Bilby, D.; Amonoo, J.; Sykes, M. E.; Frieberg, B.; Huang, B.; Hungerford, J.; Shtein, M.; Green, P.; Kim, J. Reduction of Open Circuit Voltage Loss in a Polymer Photovoltaic Cell via Interfacial Molecular Design: Insertion of a Molecular Spacer. *Appl. Phys. Lett.* **2013**, *103*, 203902.
(54) Santhanamoorthi, N.; Lo, C.-M.; Jiang, J.-C. Molecular Design of Porphyrins for Dye-Sensitized Solar Cells: A DFT/TDDFT Study. *J. Phys. Chem. Lett.* **2013**, *4*, 524−530.
(55) Fu, Y.; Cha, H.; Song, S.; Lee, G.-Y.; Park, C. E.; Park, T. Low-Bandgap Quinoxaline-Based D−A-Type Copolymers: Synthesis,Characterization, and Photovoltaic Properties. *J. Polym. Sci., Part A: Polym. Chem.* **2013**, *51*, 372−382.
(56) Mercier, L. G.; Aïcha, B. R.; Najari, A.; Beaupré, S.; Berrouard, P.; Pron, A.; Robitaille, A.; Tao, Y.; Leclerc, M. Direct Heteroarylation of β-Protected Dithienosilole and Dithienogermole Monomers with Thieno[3,4-c]pyrrole-4,6-dione and Furo[3,4-c]pyrrole-4,6-dione. *Polym. Chem.* **2013**, *4*, 5252−5260.
(57) Veldman, D.; Meskers, S. C. J.; Janssen, R. A. J. The Energy of Charge-Transfer States in Electron Donor−Acceptor Blends: Insight into the Energy Losses in Organic Solar Cells. *Adv. Funct. Mater.* **2009**, *19*, 1939−1948.
(58) Perez, M. D.; Borek, C.; Forrest, S. R.; Thompson, M. E. Molecular and Morphological Influences on the Open Circuit Voltages of Organic Photovoltaic Devices. *J. Am. Chem. Soc.* **2009**, *131*, 9281−9286.
(59) Servaites, J. D.; Savoie, B. M.; Brink, J. B.; Marks, T. J.; Ratner, M. A. Modeling Geminate Pair Dissociation in Organic Solar Cells: High Power Conversion Efficiencies Achieved with Moderate Optical Bandgaps. *Energy Environ. Sci.* **2012**, *5*, 8343−8350.
(60) Yao, Y.; Hou, J.; Xu, Z.; Li, G.; Yang, Y. Effects of Solvent Mixtures on the Nanoscale Phase Separation in Polymer Solar Cells. *Adv. Funct. Mater.* **2008**, *18*, 1783−1789.
(61) Watts, B.; Belcher, W. J.; Thomsen, L.; Ade, H.; Dastoor, P. C. A Quantitative Study of PCBM Diffusion during Annealing of P3HT:PCBM Blend Films. *Macromolecules* **2009**, *42*, 8392−8397.
(62) Schaffer, C. J.; Palumbiny, C. M.; Niedermeier, M. A.; Jendrzejewski, C.; Santoro, G.; Roth, S. V.; Müller-Buschbaum1, P. A Direct Evidence of Morphological Degradation on a Nanometer Scale in Polymer Solar Cells. *Adv. Mater.* **2013**, *25*, 6760−6764.
(63) Mikhnenko, O. V.; Azimi, H.; Scharber, M.; Morana, M.; Blom, P. W. M.; Loi, M. A. Exciton Diffusion Length in Narrow Bandgap Polymers. *Energy Environ. Sci.* **2012**, *5*, 6960−6965.
(64) Luhman, W. A.; Holmes, R. J. Investigation of Energy Transfer in Organic Photovoltaic Cells and Impact on Exciton Diffusion Length Measurements. *Adv. Funct. Mater.* **2011**, *21*, 764−771.
(65) Collins, B. A.; Li, Z.; Tumbleston, J. R.; Gann, E.; McNeill, C. R.; Ade, H. Absolute Measurement of Domain Composition and Nanoscale Size Distribution Explains Performance in PTB7:$PC_{71}BM$ Solar Cells. *Adv. Energy Mater.* **2013**, *3*, 65−74.
(66) Yu, S.; Santoro, G.; Sarkar, K.; Dicke, B.; Wessels, P.; Bommel, S.; Döhrmann, R.; Perlich, J.; Kuhlmann, M.; Metwalli, E.; Risch, J. F. H.; Schwartzkopf, M.; Drescher, M.; Müller-Buschbaum, P.; Roth, S. V. Formation of Al Nanostructures on Alq3: An in Situ Grazing Incidence Small Angle X-ray Scattering Study during Radio Frequency Sputter Deposition. *J. Phys. Chem. Lett.* **2013**, *4*, 3170−3175.
(67) Kaune, G.; Metwalli, E.; Meier, R.; Körstgens, V.; Schlage, K.; Couet, S.; Röhlsberger, R.; Roth, S. V.; Müller-Buschbaum, P. Growth and Morphology of Sputtered Aluminum Thin Films on P3HT. *ACS Appl. Mater. Interfaces* **2011**, *3*, 1055−1062.
(68) Credgington, D.; Jamieson, F. C.; Walker, B.; Nguyen, T.-Q.; Durrant, J. R. Quantification of Geminate and Non-Geminate Recombination Losses within a Solution-Processed Small-Molecule Bulk Heterojunction Solar Cell. *Adv. Mater.* **2012**, *24*, 2135−2141.
(69) Kirchartz, T.; Pieters, B. E.; Kirkpatrick, J.; Rau, U.; Nelson, J. Recombination via Tail States in Polythiophene:Fullerene Solar Cells. *Phys. Rev. B* **2011**, *83*, 115209.
(70) Credgington, D.; Hamilton, R.; Atienzar, P.; Nelson, J.; Durrant, J. R. Non-Geminate Recombination as the Primary Determinant of Open-Circuit Voltage in Polythiophene:Fullerene Blend Solar Cells: an Analysis of the Influence of Device Processing Conditions. *Adv. Funct. Mater.* **2011**, *21*, 2744−2753.
(71) Keivanidis, P. E.; Kamm, V.; Zhang, W.; Floudas, G.; Laquai, F.; McCulloch, I.; Bradley, D. D. C.; Nelson, J. Correlating Emissive Non-Geminate Charge Recombination with Photocurrent Generation Efficiency in Polymer/Perylene Diimide Organic Photovoltaic Blend Films. *Adv. Funct. Mater.* **2012**, *22*, 2318−2326.
(72) Mangold, H.; Bakulin, A. A.; Howard, I. A.; Kästner, C.; Egbe, D. A. M.; Hoppe, H.; Laquai, F. Control of Charge Generation and Recombination in Ternary Polymer/Polymer:Fullerene Photovoltaic Blends using Amorphous and Semi-crystalline Copolymers as Donors. *Phys. Chem. Chem. Phys.* **2014**, DOI: 10.1039/c4cp01883d.
(73) Zhou, H.; Yang, L.; Stoneking, S.; You, W. A Weak Donor−Strong Acceptor Strategy to Design Ideal Polymers for Organic Solar Cells. *ACS Appl. Mater. Interfaces* **2010**, *2*, 1377−1383.
(74) Yum, S.; An, T. K.; Wang, X.; Lee, W.; Uddin, M. A.; Kim, Y. J.; Nguyen, T. L.; Xu, S.; Hwang, S.; Park, C. E.; Woo, H. Y. Benzotriazole-Containing Planar Conjugated Polymers with Non-covalent Conformational Locks for Thermally Stable and Efficient Polymer Field-Effect Transistors. *Chem. Mater.* **2014**, *26*, 2147−2154.